Simplification and Cost Reduction of Visual Corona Tests

J.-R. Riba[1*], C. Abomailek[1], P. Casals-Torrens[1], and F. Capelli[2]
[1]Electrical Engineering Department, Universitat Politècnica de Catalunya, 08222 Terrassa, Spain
[2]SBI Connectors Spain SAU, 08635 Sant Esteve Sesrovires, Spain
*Corresponding author: riba@ee.upc.edu

Abstract: Visual corona tests are useful to identify the critical corona points of substation connectors and other high-voltage components, thus allowing to apply corrective actions. RIV (radio interference voltage) and PD (partial discharge) measurements also allow detecting corona activity. However, these techniques require expensive screened laboratories, sophisticated instrumentation and usually do not provide the exact location of the discharges. Corona tests are often performed in external and expensive laboratories, where customers habitually have to face long waiting times. The tests in such laboratories must be totally planned beforehand, as they are habitually done by external engineers, so little information about the behavior and possible modifications of the product is acquired by the customer. This paper proposes a feasible solution to perform routine corona tests for product optimization in industrial facilities, while greatly reducing the voltage applied, the laboratory size and requirements, assembly and testing times, and thus the test related costs. In addition, this paper detects the visual corona onset by means of a commercial digital camera, which allows locating the critical corona points, thus greatly decreasing the costs of the corona detection instrumentation, while maintaining the accuracy and sensitivity of the detection method. The methodology proposed in this paper can be applied to many other high-voltage devices such as conductors, spacers for bundle conductors, vibration dumpers, corona protections, and different types of hardware and fittings for power lines and substations.

Keywords: corona inception voltage, corona extinction voltage, visual corona, finite element method, substation connector.

1. INTRODUCTION

Components for high-voltage applications such as substation connectors must be free of corona for the specified conditions of operation. Corona is a type of partial discharge that produces a localized ionization of the gaseous insulation surrounding an energized electrode, when the voltage gradient exceeds a critical onset value [1], [2]. Corona can also be understood as the release of capacitive energy stored in the electric field [3]. Two regions characterize corona discharges, a thin ionizing layer, which surrounds the outer surface of the active electrode, and a drift region, in which the field drives the ions towards the collecting electrode. The thin ionizing layer is often considered as a unique source of unipolar ions, which generate a space charge density and travel along the field lines [4]. The micro-physical processes of gas discharge that lead to corona are often expressed in terms of ionization by collision, drift of ionic particles, photoionization, attachment and recombination processes [5].

Corona discharges are a focus of concern in high-voltage power systems due to their harmful effects such as ozone generation, audible noise, electromagnetic interference and power loss [2], [6]–[9]. They tend to occur at sharp protrusions from electrodes in gases and liquid insulation systems [10]. Corona current pulses are very fast, thus being a main source of wide-spectral-range electromagnetic interference, covering from the ultraviolet and visible to radio and TV spectral regions [11]. Corona discharges can also produce voltage transients and degrade insulation systems, since their effects are permanent and cumulative [12], thus reducing the reliability of power systems. Corona discharges are invisible in daylight because most of the radiation falls within the ultraviolet spectrum, thus being almost imperceptible to the human eye. Consequently, visual corona is often detected in total darkness or through specialized measurements

involving audible noise or electromagnetic radiation [13], including partial discharge (PD) detectors, ultraviolet imagers, sound level meter and radio interference voltage (RIV) receivers [9].

Visual corona tests are useful to identify the weak points of high-voltage components, and thus corrective actions can be applied during their optimal design stage. The accurate detection and assessment of the corona onset conditions plays an important role when designing high-voltage devices [2], [3], [7], [14], [15]. RIV and PD measurements also allow detecting corona activity. However, these techniques do not give the exact location of the discharge points. Several international standards deal with PD, RIV, and visual corona detection methods, such as the NEMA 107-2016 (RIV) [16], the IEC 60270:2000 (PD) [17], the IEEE Std. 1829-2017 (visual corona and RIV) [18] or the ANSI/NEMA CC1-2009 (visual corona and RIV) [19], the last one is specific for substation connectors. The RIV level is expressed in μV, according to the human ear acoustical noise impression. This is a drawback of the RIV method, as it is not directly related to the PD activity [20]. The PD activity, as measured by the IEC 60270:2000 [17], is related to the apparent charge, expressed in pC [20], that is, the charge that if injected suddenly between the test object terminals, would transitorily alter the voltage between the terminals by the same amount as done by the partial discharge [1].

Standard corona tests usually require large-size high-voltage laboratory facilities which are scarce, since fully screened high-voltage laboratories including all research and test equipment and facilities cost several millions of US dollars [21]. Therefore, industry is often forced to perform the standard corona tests in external and expensive laboratories, in which customers habitually have to face long waiting times. These tests tend to be very rigid and must be totally planned in advance, since they are carried out by the personnel of the external laboratory, with almost no intervention of the customer's engineers. Therefore, very little information about the behavior and possible modifications of the product is acquired by the customer.

This paper proposes a feasible solution to perform routine corona tests for product optimization in industrial unscreened laboratories with a voltage limit in a range of 100-150 kV_{RMS}, which requires a financially affordable high-voltage generator and a reduced size of the testing area. This strategy allows a significant reduction of assembly and testing times, the requirements of the high-voltage generator and the associated measuring instruments, the size of the laboratory and the overall test costs. In addition, the visual corona inception and extinction conditions are detected by means of a commercial digital camera, which allows locating the points more prone to corona appearance. The use of such camera greatly decreases the cost and requirements of the visual corona detection instrumentation, while almost maintaining the accuracy and sensitivity of the detection method compared to RIV and PD measurements, as proved in Section 4**.**

The proposed system is aimed at reducing the height of the test object above the ground plane during the experiments. This strategy allows a drastic reduction of both the corona inception and extinction voltages, and greatly simplifies the assembling of the experimental setup. The proposed approach requires performing FEM (finite element method) simulations to calculate the voltage gradient of the critical corona points by analyzing the same geometry as in the standard experimental corona test. Next, again through FEM simulations, the connector is simulated, and afterwards tested at a reduced height above the ground plane, in a small-size laboratory. The voltage to be applied so that the critical corona points have the same voltage gradient as in the standard corona test is determined. The proposed system is very useful, especially in the design and optimization phase of substation connectors. When obtaining unacceptable results, this procedure is iterated by modifying the geometry of the connector until satisfactory results are obtained. Finally, the optimized design must pass the mandatory standard corona test in the external laboratory.

Although the approach proposed in this paper has been applied to the analysis of substation connectors, it can be generalized to many other high-voltage devices such as conductors, spacers for bundle conductors, vibration dumpers, corona protections, or line and substation fittings among others.

2. THE APPROACH PROPOSED IN THIS PAPER

This section describes the approach proposed in this work to perform simplified visual corona tests for

product optimization at industrial laboratory level, that is, in the facilities of the manufacturer. It allows a drastic reduction of the requirements in terms of laboratory size, maximum voltage, nominal power, and instrumentation compared with those required in standard corona tests. In addition, the high-voltage generator required for the visual corona tests does not necessarily require to be free of partial discharges, thus greatly reducing its cost. The strategy proposed can be summarized in three basic steps, which are detailed below.

The first step (Step 1.1 in Fig. 1) consists in performing a FEM simulation of the standard corona test. The geometry to simulate must be the same as in the standard test, which is usually performed in a large-size screened high-voltage laboratory, with the test object (the substation connector) placed at several meters above the ground plane, as shown in Table 1. The voltage applied must be the same as that in the standard corona test, that is, at least 10% above the nominal operating voltage of the test object [19]. Corona can be simulated by applying different approaches. One of the most widely used is the FEM method [4], [7]. FEM simulations allow locating the most stressed or critical points of the connector surface, and determining the voltage gradient of such points. The objective of this process is to locate the critical corona points on the surface of the connector and to calculate their electric field strength, to determine the voltage that should be applied in the reduced-height test while maintaining the same voltage gradient on the critical corona points (see Step 1.2). Next (Step 1.2 in Fig. 1), FEM simulations are carried out maintaining the basic geometry of the problem, but reducing significantly the height of the test object above the ground plane (typically less than 1 m) and the voltage applied. The critical corona points will be the same as in the previous step. The test voltage to be applied in the simplified experimental visual corona test in Step 2 is obtained from the FEM simulations, so that the voltage gradient of the critical points during the simplified visual corona test, calculated, is the same as that in Steps 1.1 and 1.2.

The second step (Step 2 in Fig. 1) refers to the simplified visual corona test carried out in a small-size unscreened laboratory, using a digital camera to detect the critical corona points of the connector surface. The test object is placed at the reduced height above the ground plane calculated in Step 1.2. This test has several advantages, since the engineers responsible for designing and optimizing the product perform the test in the manufacturer's laboratory, so there is no need to face long waiting times. Moreover, this strategy allows gathering many useful product information, thus facilitating a further optimization of the connector in case it does not fulfill the requirements, that is, when detecting visual corona activity. Steps 1 and 2 allow applying an iterative approach until visual corona activity is completely eliminated. Once in that point, it is assumed that the connector is ready to pass the standard corona test.

The third step consist in conducting the mandatory standard corona test in a large-size high-voltage screened external laboratory. In this case, the test object will be placed at several meters above ground plane and both visual and RIV or PD standard measurement will be carried out.

Fig. 1 summarizes the three-step approach proposed in this paper.

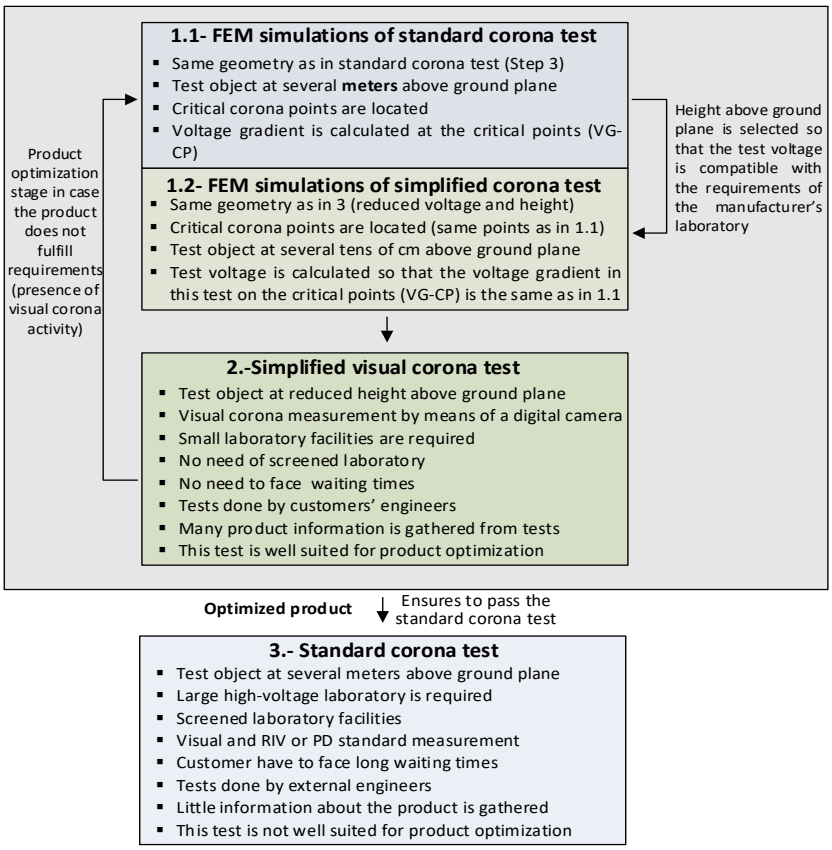

Fig. 1. Summary of the three-step approach proposed in this paper.

It is worth noting that the approach proposed in Fig. 1 is well suited during the optimal design of substation connectors and other high-voltage devices, since it ensures that the final design will pass the mandatory standard corona test.

3. FEM SIMULATIONS

This paper performs three-dimensional FEM simulations (3D-FEM) to determine the voltage gradient in the surface of the analyzed connectors. Since the experimental geometry is already known, it is introduced in the FEM software to determine the points of the connector with the highest voltage gradient, that is, those susceptible of corona appearance. The analyzed three-dimensional geometric models are simplified and prepared to reduce their complexity and expediting the simulation step, while trying to preserve their accuracy. The three-dimensional meshes dealt with are composed of tetrahedral elements. Meshes of the analyzed models consist of 3.1-8.2 x 10^6 domain elements, 4.1-6.6x10^5 boundary elements, and 4.5-6.7x10^4 edge elements depending on the simulation model applied.

The voltage gradient in the points of the analyzed domain can be determined by applying the Poisson's equation [23]. By assuming that the permittivity ε is spatially constant in the region under study, the Gauss law results in,

$$\vec{\nabla}\cdot\vec{E} = \rho / \varepsilon \tag{1}$$

where E (V/m) is the electric field and ρ (C/m^3) is the charge density. Since $\vec{E} = -\vec{\nabla}\cdot U$, U (V) being the scalar electrical potential, (1) yields the Poisson's equation for electrostatics,

$$\nabla^2 V = -\rho/\varepsilon \tag{2}$$

Finally, the electric potential and the electric field in the points within the analyzed area are found by solving (2).

FEM simulations of relatively small-size connectors placed in large-size laboratories lead to an almost

unbounded problem, that is, the field extends very far away from the connector, thus requiring a large simulation domain. This type of simulations require a large number of mesh elements, demanding computational burden and resources, thus increasing the difficulty to mesh the geometry because of the notorious size differences between the smallest and largest mesh elements. To reduce the computational burden, the infinite element domain condition has been applied. It truncates or reduces the modeled domain by adding an additional layer (a cubic box of 4 m side in this case) outside the modeled domain and applying a coordinate stretching within this domain, the solution being the same as in the real domain [23].

Fig. 2 shows the meshes of the analyzed domains for the substation connectors analyzed in this work.

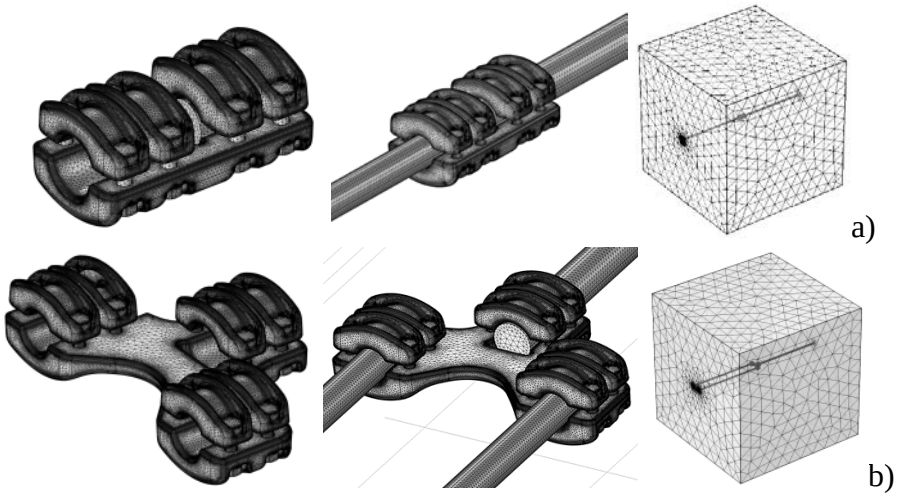

Fig. 2. Substation connectors analyzed. Geometry and meshes applied in the FEM simulations. a) Connector J40S33PK. b) Connector J40S33D4PK.

4. CALIBRATION OF THE DIGITAL CAMERA AGAINST PD MEASUREMENTS

The objective of this section is to prove that the digital camera can replace PD or RIV measurements to detect the corona onset voltage for internal industrial tests in unscreened laboratories intended for product optimization.

This section describes the tests carried out to check the sensitivity of a commercial digital camera compared to that of a commercial PD detector system. The PD system is taken as a reference, since, except in the US, it is more popular than the RIV system, and because PD measurements often provide a higher sensitivity [24], [25] due to the wider bandwidth and lower measuring frequency, thus resulting in a stronger PD signal. The main differences between the PD and RIV methods are found in the calibration procedure, the instrumentation used, and the measuring bandwidths and frequencies [25].

Rod-plane and needle-plane electrode configurations have been widely applied [26] and are considered as a reference to determine the inception voltage in air, and especially for airgaps of length beyond 0.5 m [27], to avoid unexpected flashovers. A needle-plane configuration was used to generate corona discharges, as shown in Fig. 3a. Such discharges were measured simultaneously by means of a digital camera and a PD detector, thus allowing to compare the sensitivity of both systems under the specified testing conditions.

The tests here described were carried out in a small-size laboratory of the Universitat Politècnica de Catalunya (4 m x 6.75 m, and height 3 m). A 130 kV BK-130 high-voltage generator from Phenix technologies was used to generate the test voltage. Fig. 3b shows the layout used to carry out this test.

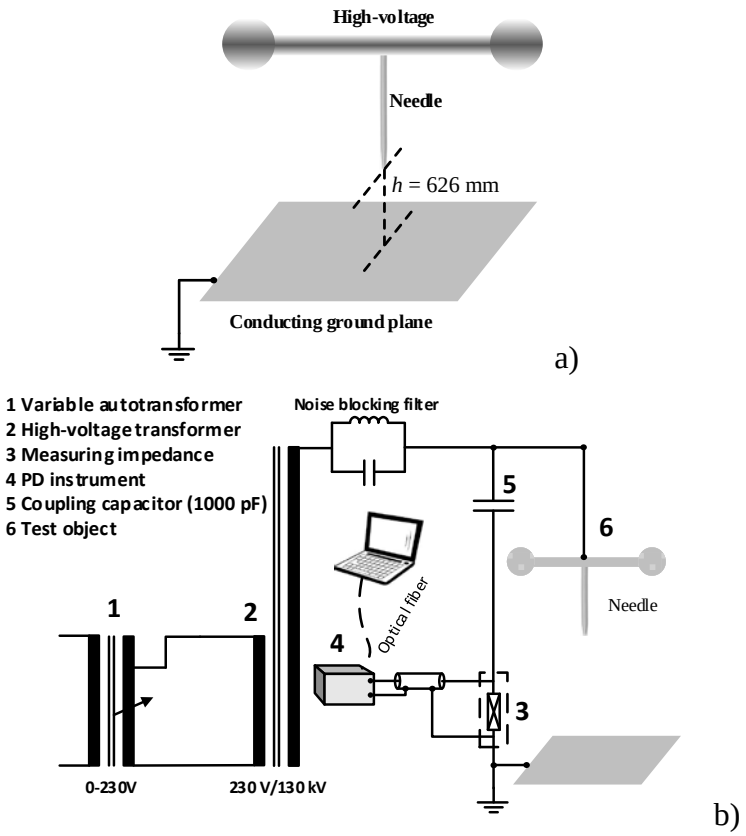

Fig. 3. a) Needle-plane experimental setup to calibrate the digital camera against PD measurements. The rod of the needle has a diameter of 3 mm, whereas the diameter of the tip is 1.5 mm. The distance between the tip of the needle and the ground plane is 626 mm. b) PD measuring circuit in accordance with the IEC60270 standard.

A Canon EOS-70D digital camera was used to detect the visual corona, which is equipped with a CMOS APS-C sensor (22.5 x 15 mm) with 20.2 Mpixels resolution and variable sensitivity in the range 100-12800 ISO. To magnify the test object an 18-135 mm lens was used. This camera incorporates the bulb mode, which allows controlling both the aperture and shutter speed. Photographs were taken with an exposition of 60 seconds, with an aperture of f/5.6, ISO-200 sensitivity, and tungsten color temperature.

PD pulses were acquired by means of a commercial Techimp PD-BaseII instrument, using the standard IEC60270 bandwidth (115-440 kHz) and a sampling frequency of 200 Msamples/s. The PD detector allows expressing the measured voltage as equivalent charge in pC. The test object was previously calibrated by means of a PDCAL PD calibrator by calculating the average value of 2000 calibration pulses to reduce the effect of the background noise.

The PD tests were carried out at local atmospheric conditions (17.1 ºC, 49.2 %RH and 987.1 hPa). Under the conditions above, the detection limit of the digital camera was 9.8 kV_{RMS} as shown in Fig. 4a. The detection limit of the PD detector was 10 kV_{RMS} with the IEC60270 bandwidth, as shown in Fig. 4b, although at 9.7 kV_{RMS} there was some corona activity, but masked by the noise-level.

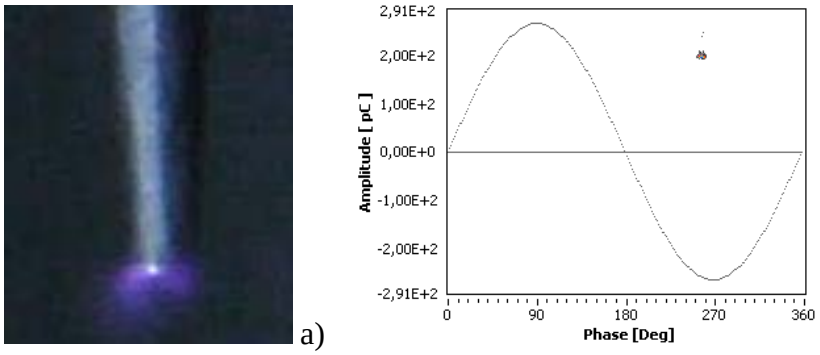

Fig. 4. Detection limit of the needle-plane setup. a) Alternating current negative corona photograph taken with the digital camera. b) Partial discharge pattern corresponding to negative corona acquired during 39.55 s (310 pulses) with the PD detector.

PD results from Fig. 4b clearly show a corona pattern, since they are concentrated in the negative semi-period of the voltage waveform, with an average phase angle of 258º.

These results suggest that the sensitivity of the digital camera is comparable to that of the PD detector under unscreened laboratory conditions. Therefore, the digital camera can be used to detect the corona activity and identify the exact location of the discharge points for routine visual corona tests intended for product optimization in industrial laboratory facilities, while reducing drastically the cost of the corona detector and facilities required. Manufacturers usually let a wide safety margin for the voltage gradient, since substation connectors are often designed to attain a voltage gradient below 2 kV_{peak}/mm which is well below the usual onset value, so a minor sensitivity difference between the digital camera and the PD detector is not significant at product optimization level.

5. EXPERIMENTAL RESULTS

Visual corona tests, which are carried out in a completely darkened laboratory, apply visible methods to identify the corona onset. Negative corona, which is produced during the negative half-cycle of the voltage produces very little corona light, audible noise and RIV, since these effects are associated to positive corona [28]. It is known that for air gaps larger than 20 mm under alternating power frequency conditions, negative corona appears first when gradually raising the voltage, although it almost does not generate acoustic noise, light and very little RIV [18]. Contrarily, positive corona produces more acoustic noise and light since it generates corona streamers of several cm length and the RIV level experiments a sudden increase. However, breakdown under positive voltage occurs at significantly lower voltage than under negative voltage. Therefore, the breakdown of non-uniform field gaps under alternating power frequency is produced during the positive half-cycle of the voltage wave [29].

Both the corona inception and extinction voltages are measured during visual corona tests. Whereas the corona inception voltage is the lowest voltage at which continuous corona happens when gradually increasing the applied voltage, the corona extinction voltage is the highest voltage at which continuous corona no longer occurs when gradually decreasing the applied voltage from beyond the corona inception value [1]. The corona inception voltage is higher than the corona extinction voltage.

This paper follows the visible corona test procedure suggested in the IEEE 1829-2017 guide [18]. First, the voltage is increased at a rate of about 2 kV/s according to the requirements of the IEEE Std 4-2013 standard [31], until observing positive corona on the test object, this being the visual corona inception voltage (CIV). Next, the voltage is increased by 10% and maintained during 1 minute. Then, the voltage is lowered slowly to determine the extinction of the positive corona (CEV). This procedure is repeated three times and a photographic report is performed. The test object passes the test when both the visual extinction and inception voltages are higher than the designed CIV and CEV thresholds, so the test object should have no visual corona activity within the range of normal operating voltage [18]. It is worth noting that this paper

deals with the CEV, since under alternating current conditions it is usually lower than the CIV.

It is known that the corona onset voltage is affected by the local atmospheric conditions [3]. It decreases with the decrease of atmospheric pressure, although this effect declines when increasing the absolute humidity, especially when the absolute humidity increases from 5 to 15 g/m^3 [30]. Therefore, when dealing with arbitrary atmospheric conditions, the voltages must be corrected to take into account this effect. In this document the voltages measured under arbitrary atmospheric conditions are transformed to those corresponding to the standard reference atmosphere (20 ºC, 101.3 kPa, and absolute humidity 11 g/m^3), according to the procedure detailed in the IEEE Std 4-2013 standard [31].

Substation connectors must be tested respecting the phase spacing and distance to ground summarized in Table 1, according to the ANSI/NEMA-CC1 standard. Both, the visual corona and audible noise extinction voltage must be at least 10% above the rated or nominal operating voltage, and the RIV level must be below 200 μV at this voltage [19]. It is noted that a RIV requirement of zero is not practical since virtually all hardware presents some measureable RIV near the operating voltage [18].

TABLE 1
PHASE SPACING AND HEIGHT ABOVE GROUND AS A FUNCTION OF THE NOMINAL OPERATING VOLTAGE ACCORDING TO ANSI/NEMA CC1-2009 [19]

Nominal voltage (kV_{RMS})	Phase spacing (m)	Height above ground plane (m)
230	3.4	4.6
345	4.9	7.6
500	7.6	9.1
765	13.7	13.7
1100	16.8	16.8

5.1 Connector J40S33PK

This section details the tests performed to the J40S33PK mechanical substation connector from SBI Connectors catalogue, which is made of A356 aluminum alloy.

To validate the suitability of the approach proposed in this paper, at first, the standard corona test was carried out. To this end, the J40S33PK mechanical substation connector was tested at the facilities of Veiki Laboratory (Budapest, Hungary) by means of RIV measurements. The J40S33PK substation connector was placed at 7 m height above the ground plane level. The measured corona extinction voltage was about 170 kV_{RMS}, with a RIV level of 71 μV, which is below the 200 μV limit value suggested by the ANSI/NEMA-CC1. Therefore the tests are done applying more restrictive conditions than those imposed by the ANSI/NEMA-CC1 standard. RIV measurements were performed at 0.65 MHz across a 300 Ω impedance in accordance with the IEC 60437 standard [32]. The connection diagram is similar to that in Fig. 3b, but replacing the measuring impedance by another one in accordance with the requirements of the ANSI/NEMA CC1-2009 and using a RIV meter (Siemens B83600-B40). The test was carried out at local atmospheric conditions, 25.2 ºC, 998 hPa and 53.6% relative humidity.

Next, the standard experimental test was replicated by means of FEM simulations, reproducing the same geometry, following the procedure detailed in Section 2. The simulations allowed determining the critical corona points on the surface of the connector and the voltage gradient in such points during the corona extinction conditions, as shown in Fig. 5.

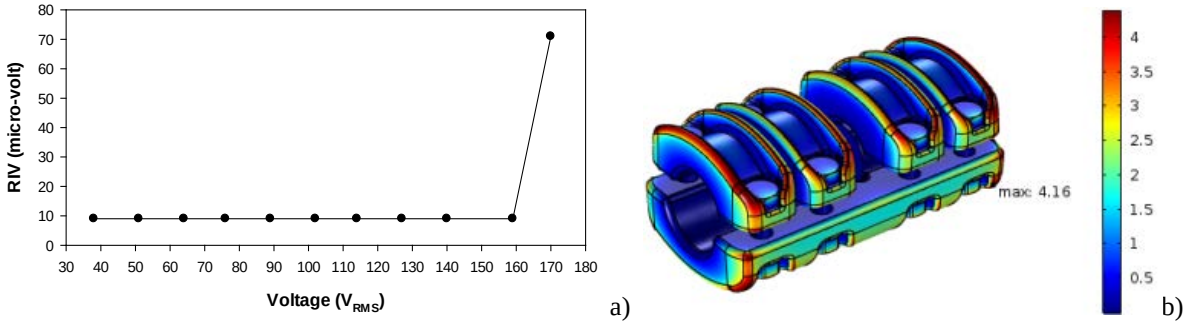

a) b)

Fig. 5. Connector J40S33PK. Large-size screened laboratory. The height above ground plane is 7 m. a) RIV measurement to determine the corona inception voltage conducted in Veiki Laboratory. b) FEM simulation. The electric field strength is given in kV_{peak}/mm.

Next, FEM simulations were performed by preserving the geometry of the problem but decreasing significantly the height of the J40S33PK connector above the ground plane to 0.315 m. This height was selected to ensure corona onset conditions below 130 kV_{RMS}, which is the maximum voltage of the small-size laboratory dealt with in this work (see Section 4). It was verified that the critical corona points on the surface of the connector under these new conditions were the same as in the standard corona test carried out in the large-size high-voltage laboratory.

Finally, the connector was tested in the small-size laboratory of the Universitat Politècnica de Catalunya, with the connector placed at only 0.315 m above the ground plane level. Fig. 6 shows the experimental setup, the results of the FEM simulations and the evidence of the visual corona tests.

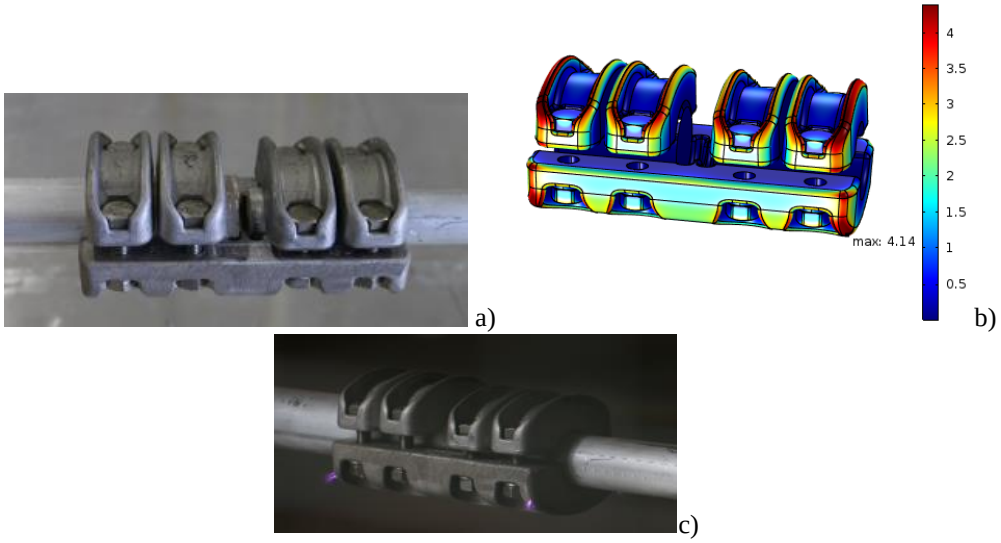

a) b)

c)

Fig. 6. Connector J40S33PK. Small-size unscreened laboratory. The height above ground plane is 0.315 m. a) Experimental setup of the simplified visual corona test including the tested substation connector, the conductors and the spherical corona protections. b) FEM simulation of the J40S33PK mechanical substation connector. The electric field strength is given in kV_{peak}/mm. c) Visual corona photographed with the digital camera.

Table 2 summarizes the results obtained in this section. It shows that the extinction voltage gradient for the visual corona tests carried out in the large-size and small-size laboratories are almost the same. These results prove the suitability of the approach applied in this paper, which allows reducing assembly and testing times, the requirements of the high-voltage generator and the measuring systems involved, the size of the laboratory and the overall test related costs.

TABLE 2
COMPARATIVE RESULTS BETWEEN LARGE-SIZE AND SMALL-SIZE LABORATORIES

Laboratory type	Corona extinction voltage* (kV_{RMS})	Extinction voltage gradient* (kV_{peak} /mm)	Height above ground plane (m)
Large-size	170	4.16	7.0
Small-size	98	4.14	0.315

*Corrected to standard atmospheric conditions according to [31].

To prove the suitability of the proposed approach, Fig. 7 compares the results of the FEM simulations when the connector is placed at a height of 0.315 m and 7 m above the ground plane. It shows that the height clearly influences the electric field distribution far from the surface of the connector. However, the distribution of surface electric field is almost the same for both configurations and therefore, the location of the critical corona points on the surface of the connector remains virtually unchanged.

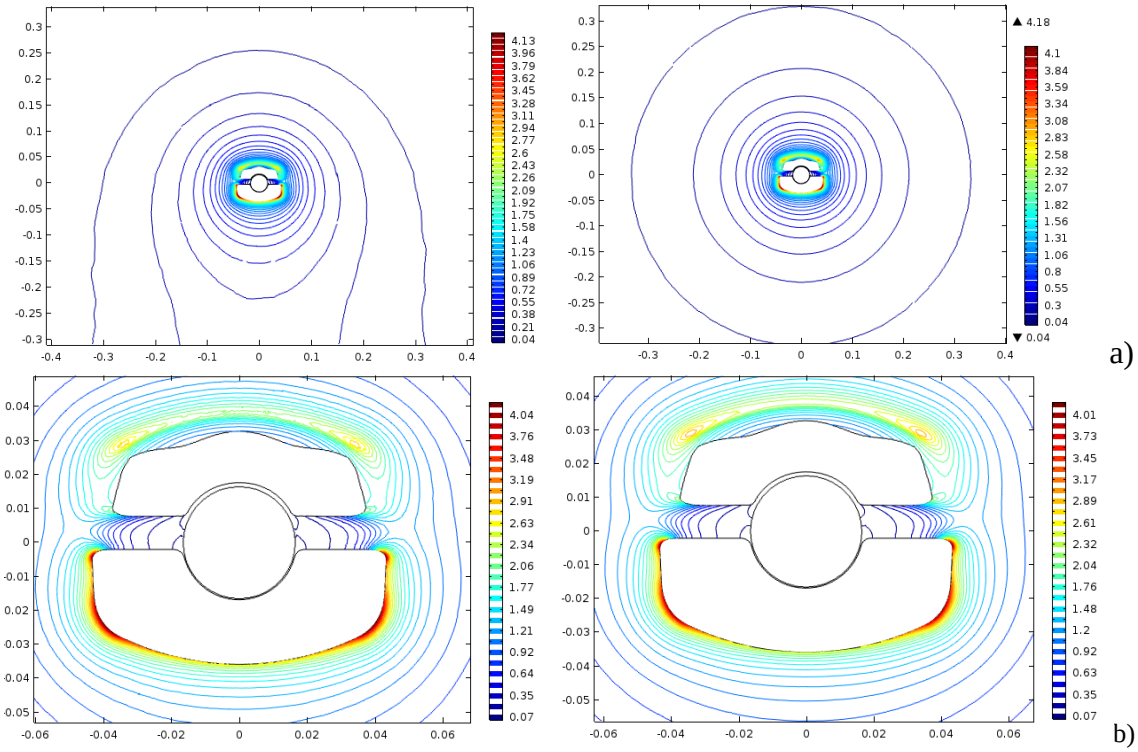

Fig. 7. a) Electric field (kV_{peak}/mm) distribution around the most stressed parts of the connector for the connector placed at a height of 0.315 m and 7 m above the ground plane, respectively. b) Detail of the electric field distribution on the vicinities of the surface of the connector for both configurations, 0.315 m and 7 m above the ground plane, respectively.

5.2 Connector J40S33D4PK

This section analyzes a second mechanical substation connector, to further validate the approach proposed in this paper. The J40S33D4PK from SBI connectors, made of A356 aluminum alloy, was also tested in the facilities of Veiki Laboratory (Budapest, Hungary). It was placed at 7 m height above the ground plane level. The laboratory, measuring devices and experimental conditions were the same as in the previous section. The measured corona extinction voltage was about 170 kV_{RMS}, corresponding to 141 μV, which is again below the 200 μV limit value suggested by the ANSI/NEMA-CC1 standard.

Next, the experimental test was replicated by means of FEM simulations, by reproducing the same geometry as in the standard test, as detailed in Section 2. FEM simulations allowed determining the critical corona points on the surface of the connector and the voltage gradient in such points during the corona

extinction conditions, as shown in Fig. 8.

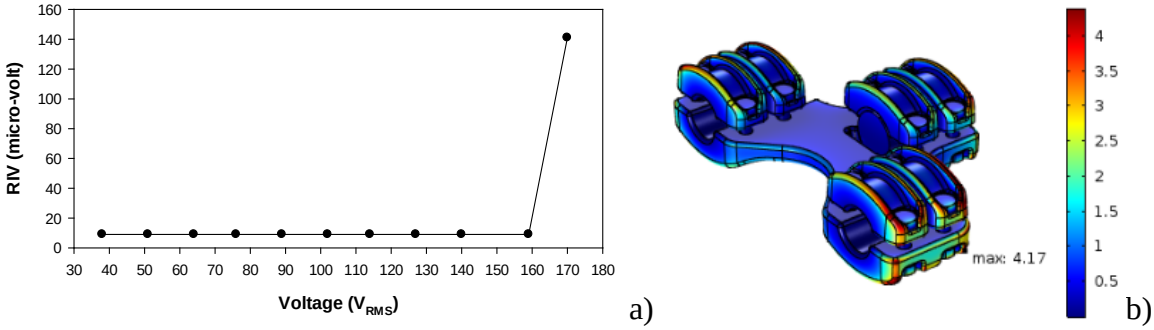

Fig. 8. Connector J40S33D4PK. Large-size screened laboratory. The height above ground plane is 7 m. a) RIV measurement to determine the corona inception voltage conducted in Veiki Laboratory. b) FEM simulation. The electric field strength is given in kV_{peak}/mm.

Next, FEM simulations were performed by preserving the geometry of the problem, but decreasing considerably the height of the J40S33D4PK connector above the ground plane to 0.455 m. This height of was selected to ensure corona onset conditions below 130 kV_{RMS}, which is the maximum voltage of the small-size laboratory dealt with in this work (see Section 4). FEM simulations verified that the critical corona points on the surface of the connector under these new conditions were the same as in the standard corona test carried out in the large-size high-voltage laboratory.

Finally, the J40S33D4PK was tested in the small-size laboratory of the Universitat Politècnica de Catalunya, with the connector placed at only 0.455 m above the ground plane, according to the results of the FEM simulations. Fig. 9 shows the experimental setup, the results of the FEM simulations and the evidence of the visual corona tests.

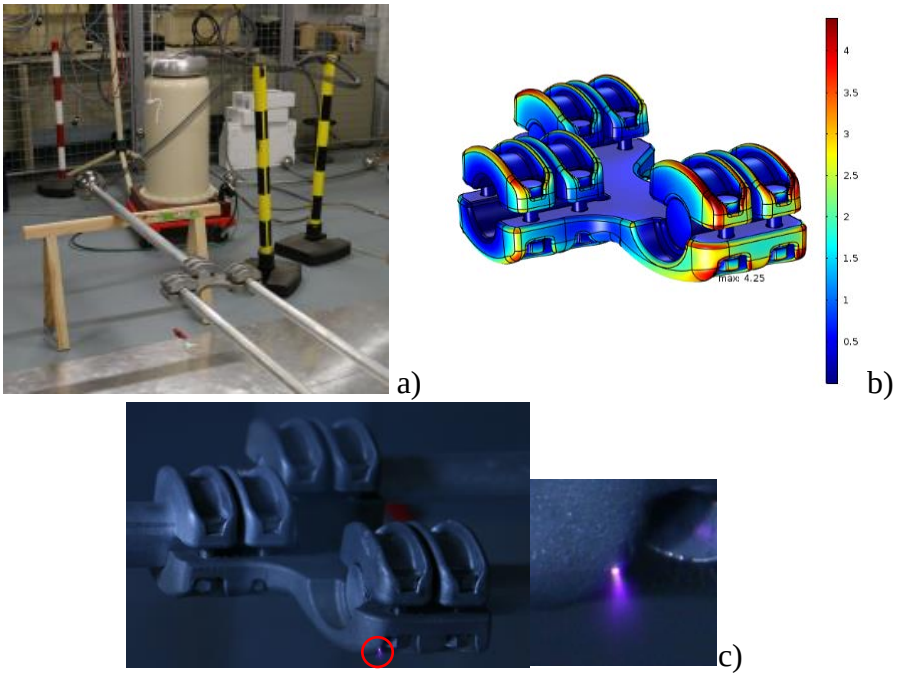

Fig. 9. Connector J40S33D4PK. Small-size unscreened laboratory**.** a) Experimental setup of the simplified visual corona test including the tested substation connector, the conductors and the spherical corona protections. The height above ground plane is 0.455 m. b) FEM simulation of the J40S33D4PK mechanical substation connector. The electric field strength is given in kV_{peak}/mm. c) Visual corona photographed with the digital camera.

Table 3 summarizes the results obtained in this section. It suggests that the extinction voltage gradient for

the visual corona tests carried out in a large-size and in a small-size laboratory are approximately the same.

TABLE 3
COMPARATIVE RESULTS BETWEEN LARGE-SIZE AND SMALL-SIZE LABORATORIES

Laboratory type	Corona extinction voltage* (kV_{RMS})	Extinction voltage gradient* (kV_{peak} /mm)	Height above ground plane (m)
Large-size	170	4.17	7.0
Small-size	101	4.25	0.455

*Corrected to standard atmospheric conditions according to the [31].

6. CONCLUSION

This paper has proposed a method to speed up, simplify and reduce the cost of visual corona tests intended to validate and optimize the behavior of substation connectors. In order to confirm experimentally the hypothesis formulated, two substation connectors have been simulated and tested in different laboratories. The proposed approach involves a combination of experimental tests and FEM simulations performed under realistic conditions. The visual corona onset has been detected experimentally by using a commercial digital camera, which allows locating the critical corona points on the surface of the connector. It also allows a drastic reduction of the cost of the instrumentation used to detect the corona, since this system offers a high accuracy and sensitivity.

It has been shown that following the approach proposed in this paper, the extinction voltage gradient for the visual corona tests performed in large-size and small-size laboratories are very similar. This indicates that the results obtained in small-scale industrial laboratories following the approach proposed in the paper can be very useful during the optimal design stage and to anticipate the behavior of the connector under the standard corona test, which must be performed in a screened large-size high-voltage laboratory.

ACKNOWLEDGMENT

The authors would like to thank SBI-Connectors Spain that supported this study by provisioning the samples and the equipment required for the experimental tests. They also thank the Spanish Ministry of Economy, Industry and Competitiveness for the financial support received under contract RTC-2014-2862-3. The authors also wish to acknowledge financial support from the Generalitat de Catalunya (GRC MCIA, Grant nº SGR 2014-101).

REFERENCES

[1] IEEE, “IEEE Std 100-2000 The Authoritative Dictionary of IEEE Standards Terms, Seventh Edition,” *IEEE Std 100-2000*. pp. 1–1362, 2000.

[2] C. Zhang, Y. Yi, and L. Wang, “Positive dc corona inception on dielectric-coated stranded conductors in air,” *IET Sci. Meas. Technol.*, vol. 10, no. 6, pp. 557–563, Sep. 2016.

[3] Z. Du, D. Huang, Z. Qiu, S. Shu, and J. Ruan, “Prediction study on positive DC corona onset voltage of rod-plane air gaps and its application to the design of valve hall fittings,” *IET Gener. Transm. Distrib.*, vol. 10, no. 7, pp. 1519–1526, May 2016.

[4] M. M. Abouelsaad, “Modelling of corona discharge of a tri-electrode system for electrostatic separation processes,” *IET Sci. Meas. Technol.*, vol. 8, no. 6, pp. 497–504, Nov. 2014.

[5] X. Zhang, K. Huang, and X. Xiao, “Modelling of the corona characteristics under damped oscillation impulses,” *IET Gener. Transm. Distrib.*, vol. 10, no. 7, pp. 1648–1653, May 2016.

[6] J. Hernandez-Guiteras, J. Riba, and P. Casals-Torrens, “Determination of the corona inception voltage in an extra high voltage substation connector,” *IEEE Trans. Dielectr. Electr. Insul.*, vol. 20, no. 1, pp. 82–88, Feb. 2013.

[7] Z.-X. Li, J.-B. Fan, Y. Yin, and G. Chen, “Numerical calculation of the negative onset corona

voltage of high-voltage direct current bare overhead transmission conductors," *IET Gener. Transm. Distrib.*, vol. 4, no. 9, p. 1009, 2010.
[8] Z. M. Al-Hamouz, M. Abdel-Salam, and A. M. Al-Shehri, "Inception voltage of corona in bipolar ionized fields-effect on corona power loss," *IEEE Trans. Ind. Appl.*, vol. 34, no. 1, pp. 57–65, 1998.
[9] L. Chen, J. M. K. MacAlpine, X. Bian, L. Wang, and Z. Guan, "Comparison of methods for determining corona inception voltages of transmission line conductors," *J. Electrostat.*, vol. 71, no. 3, pp. 269–275, Jun. 2013.
[10] E. Gulski, "Digital analysis of partial discharges," *IEEE Trans. Dielectr. Electr. Insul.*, vol. 2, no. 5, pp. 822–837, 1995.
[11] X. Cui *et al.*, "Accurate measurement of original current pulses because of positive corona in the coaxial cylindrical arrangement," *IET Sci. Meas. Technol.*, vol. 9, no. 1, pp. 12–19, Jan. 2015.
[12] E. A. Yahaya, M. Tsado Jacob, and A. A. Nwohu, "Power loss due to Corona on High Voltage Transmission Lines," *IOSR J. Electr. Electron. Eng.*, vol. 8, no. 3, pp. 14–19, 2013.
[13] A. L. Souza and I. J. S. Lopes, "Experimental investigation of corona onset in contaminated polymer surfaces," *IEEE Trans. Dielectr. Electr. Insul.*, vol. 22, no. 2, pp. 1321–1331, Apr. 2015.
[14] A. Pedersen, J. Lebeda, and S. Vibholm, "Analysis of Spark Breakdown Characteristics for Sphere Gaps," *IEEE Trans. Power Appar. Syst.*, vol. PAS-86, no. 8, pp. 975–978, Aug. 1967.
[15] A. Pedersen, "Calculation of Spark Breakdown or Corona Starting Voltages in Nonuniform Fields.," *IEEE Trans. Power Appar. Syst.*, vol. PAS-86, no. 2, pp. 200–206, Feb. 1967.
[16] NEMA, "NEMA 107-2016. Methods of Measurement of Radio Influence Voltage (RIV) of High Voltage Apparatus - NEMA." pp. 1–19, 2016.
[17] International Electrotechnical Commission, *IEC 60270:2000 High-voltage test techniques - Partial discharge measurements*, 3.0. International Electrotechnical Commission, 2000.
[18] IEEE, "IEEE Std 1829-2017 - IEEE Guide for Conducting Corona Tests on Hardware for Overhead Transmission Lines and Substations," 2017.
[19] ANSI/NEMA, "ANSI/NEMA CC1. Electric Power Connection for Substation." Rosslyn, Virginia, 2009.
[20] Eberhard Lemke *et al.*, "Guide for electrical Partial Discharge Measurements in compliance to IEC 60270," *Electra*, vol. 241, no. Technical Brochure 366, pp. 61–67, 2008.
[21] M. S. Naidu and V. Kamaraju, *High Voltage Engineering*. New York: Tata McGraw-Hill Publishing Company Limited, 1996.
[22] Comsol, "COMSOL 4.3 Multiphysics User's Guide." COMSOL, p. 1292, 2012.
[23] J. Hernández-Guiteras, J.-R. Riba, and L. Romeral, "Redesign process of a 765kVRMS AC substation connector by means of 3D-FEM simulations," *Simul. Model. Pract. Theory*, vol. 42, pp. 1–11, 2014.
[24] G. H. Vaillancourt, R. Malewski, and D. Train, "Comparison of Three Techniques of Partial Discharge Measurements in Power Transformers," *IEEE Trans. Power Appar. Syst.*, vol. PAS-104, no. 4, pp. 900–909, Jul. 1985.
[25] G. H. Vaillancourt, A. Dechamplain, and R. A. Malewski, "Simultaneous measurement of partial discharge and radio-interference voltage," *IEEE Trans. Instrum. Meas.*, vol. IM-31, no. 1, pp. 49–52, Mar. 1982.
[26] M. Abdel-Salam, N. L. Allen, and I. Cotton, "Computation of inception voltage and inception time of positive impulse corona in rod–plane gaps," *IET Sci. Meas. Technol.*, vol. 1, no. 4, pp. 179–184, Jul. 2007.
[27] N. L. Allen, M. Abdel-Salam, and I. Cotton, "Effects of temperature and pressure change on positive corona and sparkover under direct voltage in short airgaps," *IET Sci. Meas. Technol.*, vol. 1, no. 4, pp. 210–215, Jul. 2007.
[28] Electric Power Research Institute, *Transmission line reference book 345 kV and above*, 2014 Editi. Palo Alto, CA: Electric Power Research Institute (EPRI), 2014.
[29] J. Kuffel, W. S. Zaengl, and P. Kuffel, *High Voltage Engineering Fundamentals*, Second Edi.

Oxford: Newnes, 2000.
[30] Q. Hu, L. Shu, X. Jiang, C. Sun, S. Zhang, and Y. Shang, “Effects of air pressure and humidity on the corona onset voltage of bundle conductors,” *IET Gener. Transm. Distrib.*, vol. 5, no. 6, p. 621, Jun. 2011.
[31] IEEE, “IEEE Std 4-2013 (Revision of IEEE Std 4-1995) IEEE Standard for High-Voltage Testing Techniques,” *IEEE Std 4-2013 (Revision of IEEE Std 4-1995)*. pp. 1–213, 2013.
[32] IEC, “IEC 60437:1997. Radio interference test on high-voltage insulators.” International Electrotechnical Commission, Geneva, Switzerland, pp. 1–29, 1997.